



King Saud University

Arabian Journal of Chemistry

www.ksu.edu.sa
www.sciencedirect.com



ORIGINAL ARTICLE

Solid state synthesis and structural refinement of polycrystalline phases: $\text{Ca}_{1-2x}\text{Zr}_4\text{M}_{2x}\text{P}_{6-2x}\text{O}_{24}$ ($\text{M}=\text{Mo}$, $x = 0.1$ and 0.3)



Ashish Bohre ^{*}, O.P. Shrivastava, Kalpana Avasthi

Department of Chemistry, Dr. Harisingh Gour University, Sagar, MP 470003, India

Received 18 September 2012; accepted 4 April 2013

Available online 13 April 2013

KEYWORDS

CZP;
Rietveld refinement;
GSAS;
XRD and SEM

Abstract The structure of molybdenum substituted Polycrystalline calcium zirconium phosphate (CZP) was determined on the basis of crystal data of solid solutions. It was found that up to ~5.81 wt.% (~1.74 mol%), molybdenum could be loaded into CZP formulations without significant changes of the three-dimensional framework structure. The crystal chemistry of $\text{Ca}_{1-2x}\text{Zr}_4\text{M}_{2x}\text{P}_{6-2x}\text{O}_{24}$ ($\text{M}=\text{Mo}$, $x = 0.1$ and 0.3) phases has been investigated using General Structure Analysis System (GSAS) programming. The Mo substituted CZP phases crystallize in the space group R-3 and $Z = 6$. Powder diffraction data have been subjected to Rietveld refinement to arrive at a satisfactory structural convergence of R-factors. The PO_4 stretching and bending vibrations in the Infra red (IR) region have been assigned. Morphology and compositional analysis have been carried out by scanning electron microscopy (SEM) and Energy Dispersive X-ray Analysis (EDAX) of the specimens.

© 2013 Production and hosting by Elsevier B.V. on behalf of King Saud University. This is an open access article under the CC BY-NC-ND license (<http://creativecommons.org/licenses/by-nc-nd/3.0/>).

1. Introduction

Calcium zirconium phosphates are member of the so-called orthophosphate group of the $\text{NaZr}_2\text{P}_3\text{O}_{12}$ (NZP) family. Their unique structure and properties stimulated the development of

many derivative materials (Breval et al., 1998; Limaye et al., 1990, 1987). In recent years these solid solutions are receiving attention for their potential to be used as (i) ionic conductors (Goodenough et al., 1976) and (ii) host material for radio-active waste immobilization because of their structural flexibility with respect to isomorphic ionic replacements and high stability against leaching reactions (Kumar et al., 2011; Volkov and Orlova, 1996).

The NZP group is characterized by a flexible framework structure belonging to the rhombohedral system with a possibility of isomorphic replacements of various groups of elements (Chourasia et al., 2010; Fukuda and Fukutani, 2003; Senbhagaraman and Umarji, 1990). Compounds of the NZP

* Corresponding author. Tel.: +91 7582 223480; fax: +91 7582 222058.

E-mail address: ashish.bohre@gmail.com (A. Bohre).

Peer review under responsibility of King Saud University.



Production and hosting by Elsevier

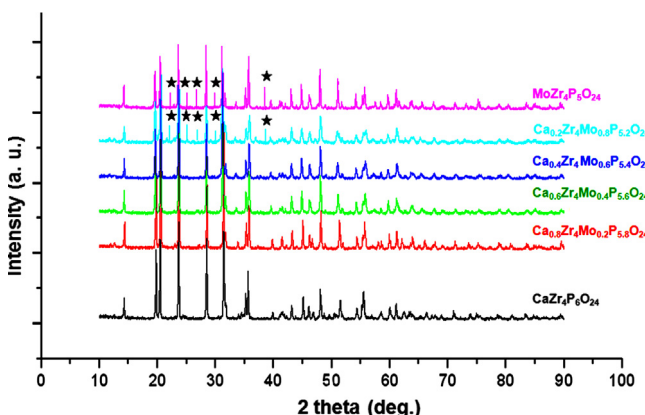


Figure 1 Powder XRD pattern of $\text{Ca}_{1-2x}\text{Zr}_4\text{M}_{2x}\text{P}_{6-2x}\text{O}_{24}$ ($\text{M}=\text{Mo}$ and $x=0.1-0.5$) ceramic samples. *Marked peaks are due to $\text{Mo}_2\text{Zr}_4\text{P}_5\text{O}_{24}$.

family (CZP, NASICON and CTP) may be represented by the general crystal-chemical formula $(\text{M}1)(\text{M}2)_3\{[\text{L}_2(\text{TO}_4)_3]^{p^-}\}_{3\infty}$. The structure consists of a network of corner sharing LO_6 octahedrons and TO_4 tetrahedrons. The structural unit consists of two octahedrons and three tetrahedrons $\{[\text{L}_2(\text{TO}_4)_3]^{p^-}\}$, which are connected in the form of ribbons parallel to the c -axis of the unit cell. These ribbons are linked together and perpendicular to the c -axis by TO_4 tetrahedrons to build the three-dimensional framework. Molybdenum having different valences is reported to occupy either L or T positions in Calcium zirconium phosphate (CZP) framework Jazouli et al., 1986; Lii et al., 1989; Shrivastava and Chourasia, 2008; Bennouna et al., 1995. Because Mo(IV) easily oxidizes in the presence of air, it is difficult to fix Mo(IV) in the L-type (Zr-site) position of CZP structure, therefore fixing of Mo atoms in T-type positions would be a favorable study for effective results. Compounds with NZP skeleton are anisotropic, changing their dimension in apposite magnitudes when the counter ion of the skeleton is substituted or thermally affected.

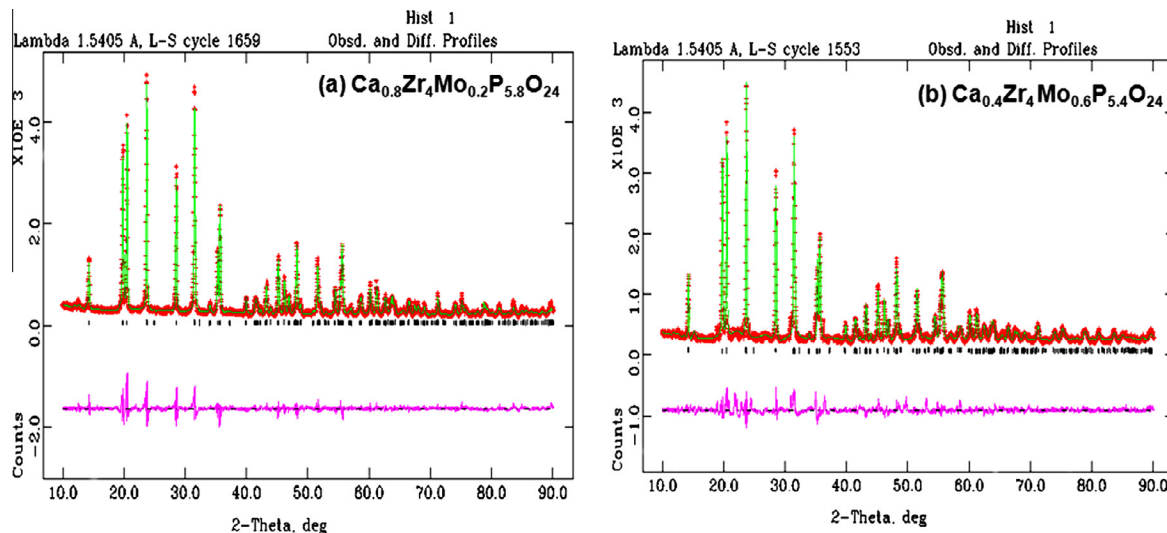


Figure 2 (a and b) Rietveld refinement plot for $\text{Ca}_{0.4}\text{Zr}_4\text{Mo}_{0.6}\text{P}_{5.4}\text{O}_{24}$ ceramic sample showing observed (+), calculated (continuous line) and difference (lower) curves. The vertical bars denote Bragg reflections of the crystalline phases.

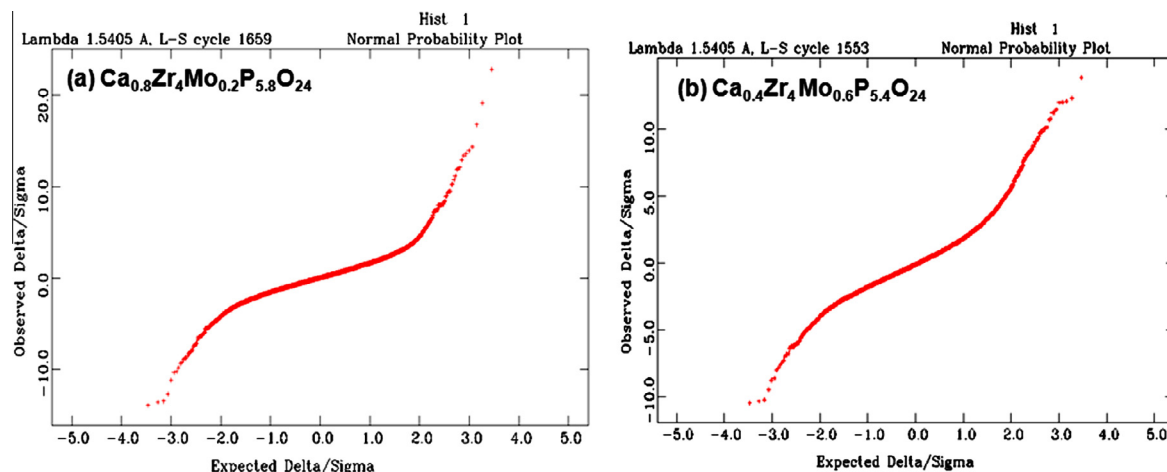


Figure 3 (a and b) Probability plot between observed intensity (I_o) and calculated intensity (I_c) for $\text{Ca}_{0.4}\text{Zr}_4\text{Mo}_{0.6}\text{P}_{5.4}\text{O}_{24}$ ceramic sample.

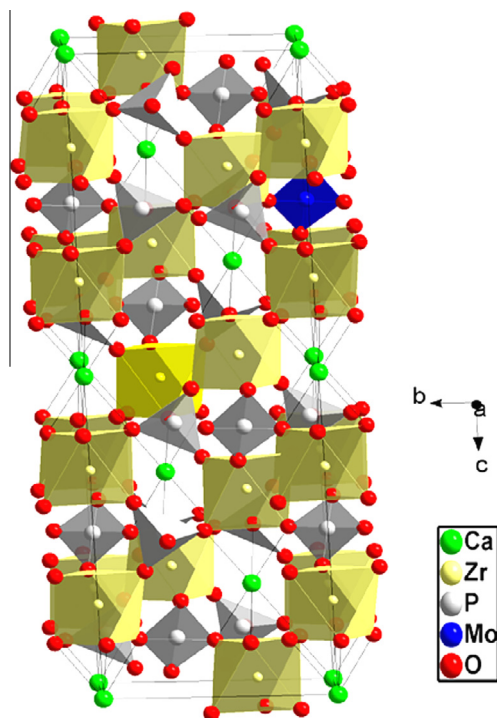


Figure 4 DIAMOND view of crystal structure of $\text{Ca}_{0.8}\text{Zr}_4\text{Mo}_{0.2}\text{P}_{5.8}\text{O}_{24}$ ceramic phase.

ble. The initial heating is done to decompose CaCO_3 , $(\text{NH}_4)_6\text{Mo}_7\text{O}_{24}$ and $(\text{NH}_4)_2\text{HPO}_4$ with the emission of carbon dioxide gases, ammonia and water vapors.

The powders were then compacted into small disks of 12.5 mm diameter and 2–3 mm of thickness under a load of four tons. Then pellets were sintered in a platinum crucible at 1250 °C for 72 h. The process was repeated to get a dense, polycrystalline material.

2.2. Characterization

The phase purity of the synthesized samples was checked by X-ray diffraction on a Pan Analytical diffractometer (XPERT-PRO) using $\text{Cu K}\alpha$ radiation ($\lambda = 1.54$) at a step size of $2\theta = 0.02^\circ$ and a fixed counting time of 5 s/step and was refined by the Rietveld method using the General Structure Analysis System (GSAS) program Agrawal and Stubican, 1985. The GSAS program with the EXPGUI (Larson and Von Dreele, 2000) graphical user interface was used to carry out crystal structure determination which allows refinement of atomic coordinates, site occupancies and atomic displacement parameters as well as profile parameters (lattice constants, peak shape, peak height, instrument parameters and background).

The homogeneity and chemical compositions of the samples were checked by Scanning electron microscopy (SEM). Scanning electron microscopy (SEM) has been carried out on a HITACHI S-3400n electron microscope system attached

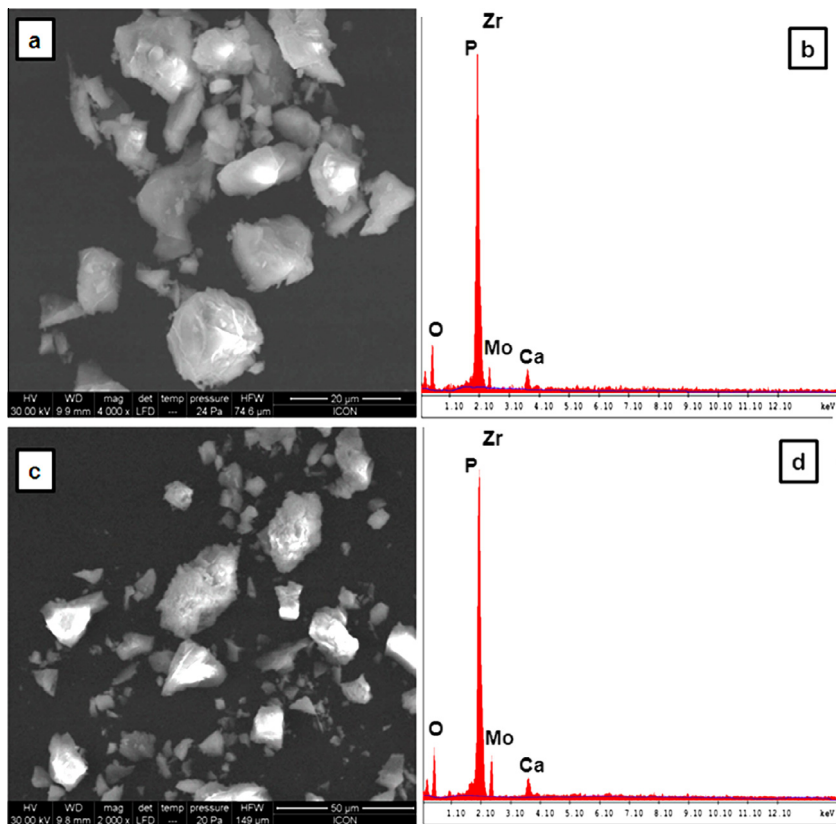


Figure 5 (a and b) Scanning electron micrographs and EDAX spectrum of $\text{Ca}_{0.8}\text{Zr}_4\text{Mo}_{0.2}\text{P}_{5.8}\text{O}_{24}$ ceramic phases. (c and d) Scanning electron micrographs and EDAX spectrum of $\text{Ca}_{0.4}\text{Zr}_4\text{Mo}_{0.6}\text{P}_{5.4}\text{O}_{24}$ ceramic phases.

Table 5 Distribution of particle size (nm) along with prominent reflecting planes of $\text{Ca}_{1-2x}\text{Zr}_4\text{M}_{2x}\text{P}_{6-2x}\text{O}_{24}$ ($x = 0.1$ and 0.3) phases.

$h k l$	$x = 0.1$	$x = 0.3$
2 0 -4	54.82	44.21
1 1 6	44.21	44.21
2 1 1	97.9	82.83
2 0 8	152.28	124.6
1 1 9	72.13	35.14
2 2 0	97.9	65.26
2 1 -8	62.3	52.17
4 0 -2	80.62	76.14
3 1 8	97.9	85.66
4 0 -8	91.37	152.28
4 1 6	72.13	152.28
3 2 10	114.21	57.10

Table 6 Assignment (cm^{-1}) of IR bands for $\text{Ca}_{1-2x}\text{Zr}_4\text{M}_{2x}\text{P}_{6-2x}\text{O}_{24}$ ($x = 0.1$ and 0.3) ceramic samples.

Compound	v_3	v_1	v_4	v_2
	v_{as} (P–O)	v_a (P–O)	δ (P–O)	(P–O)
$\text{Ca}_{0.8}\text{Zr}_4\text{Mo}_{0.2}\text{P}_{5.8}\text{O}_{24}$	1010.73			
	1030.02	904.64	520.80	410.85
	1039.67	931.65	563.23	430.14
	1172.76	985.66		443.64
	1271.13			
	1288.49			
$\text{Ca}_{0.4}\text{Zr}_4\text{Mo}_{0.6}\text{P}_{5.4}\text{O}_{24}$	1043.52	900.79	505.37	405.41
	1051.78	983.79	543.94	410.49
	1107.18	999.16	563.23	484.15
	1197.83		611.45	
			644.25	

with Thermonoran ultra dry detector facility for energy dispersive X-ray (EDAX) analysis. The images presented are recorded in backscattered electron (BSE) mode and electrons of energy 20 keV were used in all experiments. To confirm functional compositions of the phosphates, their IR spectra were recorded using a SHIMADZU FTIR-8400S instrument. Samples were prepared by finely dispersing powder material on a KBr carrier.

3. Results and discussion

3.1. Rietveld refinement and crystallographic model of the phases

The powder XRD data showed that monophases of composition $\text{Ca}_{1-2x}\text{Zr}_4\text{M}_{2x}\text{P}_{6-2x}\text{O}_{24}$ ($M = \text{Mo}$ and $x = 0.1$ and 0.3) are isostructural to $\text{CaZr}_4(\text{PO}_4)_6$ (Toby, 2001) but beyond $x = 0.3$, a secondary phase of molybdenum zirconium phosphate (marked asterisk) (International Tables for X-ray crystallography, 1984; International tables for X-ray crystallography, 1983) is evident along with CZP (Fig. 1). Mo modified CZP crystallizes in the rhombohedral system (space group $R\bar{3}$). The conditions for the rhombohedral lattice: (i) $-h + k + l = 3n$ (ii) when $h = 0, l = 2n$ and (iii) when

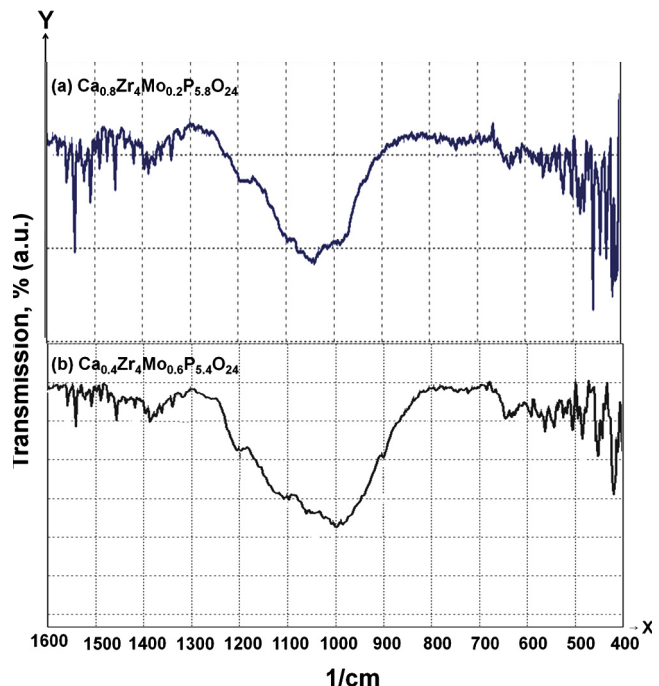


Figure 6 Infrared spectra of $\text{Ca}_{1-2x}\text{Zr}_4\text{Mo}_{2x}\text{P}_{6-2x}\text{O}_{24}$ (a) $x = 0.1$ and (b) $x = 0.3$.

$k = 0, l = 2n$ have been verified for all reflections of $2\theta = 10\text{--}90^\circ$. The intensity and positions of the diffraction pattern match with the characteristic pattern of parent compound calcium zirconium phosphate, which gives several prominent reflections of $2\theta = 12\text{--}61^\circ$ (Pet'kov et al., 2003). Ca atoms were assumed to occupy the M1 (6b) site. The occupancy of Ca(1) was allowed to vary but the total P and Mo contents were constrained and refined according to their theoretical molar ratios. The structure refinement leads to rather good agreement between the experimental and calculated XRD pattern (Fig. 2) and yields acceptable reliability factors: RF^2 , Rp and Rwp (Kojitani et al., 2005; Chourasia and Shrivastava, 2011). The normal probably plot for the histogram gives nearly a linear relationship indicating that the I_o and I_c values for the most part are normally distributed (Fig. 3). The cell parameters of the specimens register a slight increase in the c direction. Simultaneously, the structure shows a slight contraction along a direction (Table 1). This is due to angular distortions as a result of the coupled rotation of ZrO_6 and PO_4 polyhedrons (Lenain et al., 1987). Alteration in lattice parameters shows that the network slightly modifies its dimensions to accommodate the cations occupying M1 and T sites without breaking the bonds. The basic framework of CZP accepts cations of different sizes and oxidation states to form solid solutions but at the same time retaining the overall geometry unchanged. The final atomic coordinates and isotropic thermal parameters (Table 2), inter-atomic distances (Table 3) and bond angle (Table 4) are extracted from the crystal information file prepared after the final cycle of the refinement. Selected h, k, l values, d -spacing, and intensity data along with observed and calculated structure factors have been listed in Table 7. The refinement leads to acceptable Zr–O, P–O bond distances. Zr atoms are displaced from the center of the octa-

hedron due to the Ca^{2+} - Zr^{4+} repulsions. Consequently the $\text{Zr}-\text{O}(2)$ distance, neighboring the calcium $\text{Ca}(1)$, is slightly greater than the $\text{Zr}-\text{O}(1)$ distance, however, average $\text{Zr}-\text{O}$ distances are smaller than the values calculated from the ionic radii data (2.12 Å) Shannon, 1976. The $\text{O}-\text{Zr}-\text{O}$ angles vary between 79.334° and 178.120°. The angles implying the shortest bonds are superior to those involving the longest ones due to $\text{O}-\text{O}$ repulsions which are stronger for $\text{O}(1)-\text{O}(1)$ than for $\text{O}(1)-\text{O}(2)$.

The $\text{P}-\text{O}$ distances are close to those found in Nasicon type phosphates (Anantharamulu et al., 2011; Navulla, 2010). The $\text{O}-\text{P}-\text{O}$ angles vary between 107.522° and 119.055°. Fig. 4 illustrates the Diamond view showing the ZrO_6 inter ribbon distance in the structure of the title phase which is a function of amount and size of alkali cation in the M site of the 3D framework, built from ZrO_6 octahedrons and corner sharing PO_4 tetrahedrons.

3.2. SEM and EDAX analysis

The microstructure of the $\text{Ca}_{1-x}\text{Zr}_4\text{M}_{2x}\text{P}_{6-2x}\text{O}_{24}$ ($x = 0.1$ and 0.3) ceramic phases has been examined by SEM and EDAX analysis of the specimen. The morphology of MoCZP phases can be seen clearly in the electron micrographs of the ceramic sample (Fig. 5). Within the limits of experimental error, the EDAX analytical data on atomic and wt.% of Ca, Zr, P and Mo are found agreeable with their corresponding expected molar ratios. Simultaneously, the particle size was also determined using Scherrer's equation where broadening of peak is expressed as full width at half maxima in the recorded XRD pattern. The particle size varies between 35.14 and 152.28 nm (Table 5) Chourasia et al., 2010.

3.3. IR analysis

The presence of orthophosphate anions in the crystal structure was confirmed with the IR spectroscopy. Table 6 lists the IR assignments for $\text{Ca}_{1-x}\text{Zr}_4\text{M}_{2x}\text{P}_{6-2x}\text{O}_{24}$ ($x = 0.1$ and 0.3) ceramic phases. The IR spectra of CZP compounds of the formula $\text{Ca}_{1-x}\text{Zr}_4\text{M}_{2x}\text{P}_{6-2x}\text{O}_{24}$ ($x = 0.1$ and 0.3) are very similar and shown in Fig. 6. In both IR spectra, the absorption bands in the range between 1250–1022 cm⁻¹ and 650–507 cm⁻¹ are assigned to stretching and bending vibrations of $\text{P}-\text{O}$ bonds of the PO_4 tetrahedron, respectively. The stretching vibrations occur between 1270 and 1020 cm⁻¹ as ν_3 band, the symmetric stretching ν_1 and anti symmetric bending ν_4 vibrations are observed in the regions 990–900 cm⁻¹ and 640–505 cm⁻¹, respectively (Barj et al., 1983; Mbandza et al., 1985; Thomas and Andrews, 1974; Buvaneswari and Varadaraju, 1999).

4. Conclusions

Principally phase pure molybdenum containing CZP formulations can be prepared with simulated molybdenum loadings up to ~5.81 wt.% (~1.74 mol%), beyond these limits traces of the minor secondary phase of molybdenum zirconium phosphate start appearing along with the solid solution. The Rietveld plots represent a structure fit between observed and calculated intensity with satisfactory R-factors. The bond distances $\text{Zr}-\text{O}$, $\text{P}-\text{O}$, $\text{Ca}-\text{O}$ match with their corresponding values for

respective oxides. Analytical evidence allows us to conclude that molybdenum is crystallochemically fixed in the ceramic matrix.

Acknowledgements

The authors are grateful to the Department of Science and Technology (DST) New Delhi, Govt. of India for funding research project number SR/S3/ME/20/2005-SERC-Engg. in SERC scheme. Thanks are due to the department of Metturgical Engineering and Material Science I.I.T. Bombay for XRD analysis.

Appendix A

Table A1.

References

- Agrawal, D.K., Stubican, V.S., 1985. Synthesis and sintering of $\text{Ca}_{0.5}\text{Zr}_2\text{P}_3\text{O}_{12}$ -a low thermal expansion material. Mater. Res. Bull. 20, 99–106.
- Alamo, J., Roy, R., 1984. Ultralow expansion ceramics in the system $\text{Na}_2\text{O}-\text{ZrO}_2\text{P}_2\text{O}_5-\text{SiO}_2$. J. Am. Ceram. Soc. 67, C-78–C-80.
- Anantharamulu, N., Rao, K.K., Rambabu, G., Kumar, B.V., Radha, V., Vithal, M., 2011. A wide-ranging review on Nasicon type materials. J. Mater. Sci. 46, 2821–2837.
- Barj, M., Perthuis, H., Colombari, P.H., 1983. Domaines d'existence, distorsions structurales et modes de vibration des ions conducteurs dans les réseaux hôtes de type nasicon. Solid State Ionics 11, 157–177.
- Bennouna, L., Arsalane, S., Brochu, R., Lee, M.R., Chassaing, J., Quarton, M., 1995. Spécificités des ions Nb^{IV} et Mo^{IV} dans les monophosphates de type Nasicon. J. Solid State Chem. 114, 224–229.
- Breval, E., McKinstry, H.A., Agrawal, D.K., 1998. Synthesis and thermal expansion properties of the $\text{Ca}_{(1+x)/2}\text{Sr}_{(1+x)/2}\text{Zr}_4\text{P}_{6-2x}\text{Si}_{2x}\text{O}_{24}$ system. J. Am. Ceram. Soc. 81 (4), 926–932.
- Buvaneswari, G., Varadaraju, U.V., 1999. Synthesis of new network phosphates with NZP structure. J. Solid State Chem. 145, 227–234.
- Chourasia, R., Shrivastava, O.P., 2011. Crystallographic characterization and microstructure of nano ceramic powder of calcium zirconium phosphate: $\text{Ca}_{1-x}\text{M}_x\text{Zr}_4\text{P}_6\text{O}_{24}$ ($M = \text{Sr}, \text{Ba}$ and $x = 0–1$). Solid State Sci. 13, 444–454.
- Chourasia, R., Bohre, A., Ambashta, R.D., Shrivastava, O.P., Wattal, P.K., 2010. Crystallographic evaluation of sodium zirconium phosphate as a host structure for immobilization of cesium. J. Mater. Sci. 45, 533–545.
- Chourasia, R., Shrivastava, O.P., Ambashta, R.D., Wattal, P.K., 2010. Crystal chemistry of immobilization of fast breeder reactor (FBR) simulated waste in sodium zirconium phosphate (NZP) ceramic matrix. Ann. Nucl. Energy 37, 103–112.
- Fukuda, K., Fukutani, K., 2003. Crystal structure of calcium zirconium diorthophosphate, $\text{CaZr}(\text{PO}_4)_2$. In: Powder Diffir. 18 (4), 296–300.
- Goodenough, J.B., Hong, H.Y.P., Kafalas, J.A., 1976. Fast Na^+ -ion transport in skeleton structures. Mater. Res. Bull. 11, 203.
- International tables for X-ray crystallography, 1983. Natl. Bur. Stand (US) Monogr. 25, 20 17 Card no. 34-0095.
- International Tables for X-ray crystallography, 1984. Natl. Bur. Stand (US) Monogr. 25, 20, 36 Card no. 33-0321.
- Jazouli, A.E.I., Soubeiryroux, J.L., Dance, J.M., Flem, G. Le, 1986. The Nasicon-like copper (II) titanium phosphate $\text{Cu}_{0.50}\text{Ti}_2(\text{PO}_4)_3$. J. Solid State Chem. 65 (3), 351–355.

- Kojitani, H., Kido, M., Akaogi, M., 2005. Rietveld analysis of a new high-pressure strontium silicate SrSi_2O_5 . *Phys. Chem. Miner.* 32, 290–294.
- Kumar, S.P., Buvaneswari, G., Madhavan, R.R., Kutty, K.V.G., 2011. Encapsulation of heterovalent ions of two simulated high-level nuclear wastes and crystallization into single-phase NZP-based waste forms. *Radiochemistry* 53 (4), 421–429.
- Larson, A.C., Von Dreele, R.B., 2000. General Structure Analysis System technical manual, LANSCE, MS-H805. Los Almos Natl. Lab. LAUR 23, 86–748.
- Lenain, G.E., McKinstry, H.A., Limaye, S.Y., Woodward, A., 1984. Low thermal expansion of alkali-zirconium phosphates. *Mater. Res. Bull.* 19, 1451–1456.
- Lenain, G.E., McKinstry, H.A., Alamo, J., Agrawal, D.K., 1987. Structural model for thermal expansion in $\text{MZr}_2\text{P}_3\text{O}_{12}$ ($\text{M} = \text{Li, Na, K, Rb, Cs}$). *J. Mater. Sci.* 22, 17–22.
- Lii, K.H., Chen, J.J., Wand, S.L., 1989. $\text{NaMo}_2\text{P}_3\text{O}_{12}$: a new phosphate of Mo(IV). *J. Solid State Chem.* 78, 93–97.
- Limaye, S.Y., Agrawal, D.K., McKinstry, H.A., 1987. Synthesis and thermal expansion of $\text{MZr}_4\text{P}_6\text{O}_{24}$ ($\text{M} = \text{Mg, Ca, Sr, Ba}$). *Am. Ceram. Soc.* 70 (10), C-232–C-236.
- Limaye, S.Y., Agrawal, D.K., Roy, R., Mehrotra, Y., 1990. Synthesis, sintering and thermal expansion of $\text{Ca}_{1-x}\text{Sr}_x\text{Zr}_4\text{P}_6\text{O}_{24}$ – an ultra-low thermal expansion ceramic system. *J. Mater. Sci.* 26 (1), 93–98.
- Mbandza, A., Bordes, E., Courtine, P., 1985. Preparation and structural properties of the solid state ionic conductor $\text{CuTi}_2(\text{PO}_4)_3$. *Mater. Res. Bull.* 20, 251–257.
- Mentre, O., Abraham, F., Deffontaines, B., Vast, P., 1994. Structural study and conductivity properties of $\text{Ca}_{1-x}\text{Na}_{2x}\text{Ti}_4(\text{PO}_4)_6$ solid solution. *Solid State Ionics* 72, 293–299.
- Navulla, A., 2010. Semi sol-gel synthesis, conductivity and luminescence studies of $\text{Ca}_{0.5}\text{Fe}_{1-x}\text{Eu}_x\text{Sb}(\text{PO}_4)_3$ ($x = 0.1, 0.15$ and 0.2). *Solid State Ionics* 181, 659–663.
- Pet'kov, V.I., Sukhanov, M.V., Kurazhkovskaya, V.S., 2003. Molybdenum fixation in crystalline NZP matrices. *Radiochemistry* 45 (6), 620–625.
- Roy, R., Agrawal, D.K., Alamo, J., Roy, R.A., 1984. [CTP]: a new structural family of near-zero expansion ceramics. *Mater. Res. Bull.* 19, 471–477.
- Senbagaraman, S., Umarji, A.M., 1990. Effect of cation valence on thermal expansion of $\text{MTi}_2\text{P}_3\text{O}_{12}$ ($\text{M} = \text{Na, Ca}_{0.5}$, and $\text{La}_{0.33}$) compounds. *J. Solid State Chem.* 85, 169–172.
- Shannon, D., 1976. Revised effective ionic radii and systematic studies of interatomic distances in halides and chalcogenides. *R. Acta Crystallogr. A* 32, 751–767.
- Shrivastava, O.P., Chourasia, R., 2008. Crystal chemistry of sodium zirconium phosphate based simulated ceramic waste forms of effluent cations (Ba^{2+} , Sn^{4+} , Fe^{3+} , Cr^{3+} , Ni^{2+} and Si^{4+}) from light water reactor fuel reprocessing plants. *J. Hazard. Mater.* 153, 285–292.
- Thomas, D.M., Andrews, L., 1974. Matrix reactions of alkaline earth metal atoms with ozone: Infrared spectra of the metal ozonide and metal oxide molecules. *J. Mol. Spectrosc.* 50, 220–234.
- Toby, B.H., 2001. EXPGUI, a graphical user interface for GSAS. *J. Appl. Crystallogr.* 34, 210–213.
- Volkov, Ju.F., Orlova, A.I., 1996. Formula types systematics of orthophosphates of one, two, three, four and five-valence elements. *Radiochemistry* 38, 15–21.